

University of Groningen

EFFECT OF AUSTENITIC CRYSTAL ORIENTATION IN A MULTIPHASE STEEL ANALYZED BY A DISCRETE DISLOCATION-TRANSFORMATION MODEL

Shi, J.; Turteltaub, S.; Van der Giessen, E.

Published in:
International Journal of Material Forming

DOI:
[10.1007/s12289-009-0469-x](https://doi.org/10.1007/s12289-009-0469-x)

IMPORTANT NOTE: You are advised to consult the publisher's version (publisher's PDF) if you wish to cite from it. Please check the document version below.

Document Version
Publisher's PDF, also known as Version of record

Publication date:
2009

[Link to publication in University of Groningen/UMCG research database](#)

Citation for published version (APA):

Shi, J., Turteltaub, S., & Van der Giessen, E. (2009). EFFECT OF AUSTENITIC CRYSTAL ORIENTATION IN A MULTIPHASE STEEL ANALYZED BY A DISCRETE DISLOCATION-TRANSFORMATION MODEL. *International Journal of Material Forming*, 2, 435-438. <https://doi.org/10.1007/s12289-009-0469-x>

Copyright

Other than for strictly personal use, it is not permitted to download or to forward/distribute the text or part of it without the consent of the author(s) and/or copyright holder(s), unless the work is under an open content license (like Creative Commons).

The publication may also be distributed here under the terms of Article 25fa of the Dutch Copyright Act, indicated by the "Taverne" license. More information can be found on the University of Groningen website: <https://www.rug.nl/library/open-access/self-archiving-pure/taverne-amendment>.

Take-down policy

If you believe that this document breaches copyright please contact us providing details, and we will remove access to the work immediately and investigate your claim.

Downloaded from the University of Groningen/UMCG research database (Pure): <http://www.rug.nl/research/portal>. For technical reasons the number of authors shown on this cover page is limited to 10 maximum.

EFFECT OF AUSTENITIC CRYSTAL ORIENTATION IN A MULTIPHASE STEEL ANALYZED BY A DISCRETE DISLOCATION-TRANSFORMATION MODEL

J. Shi¹, S. Turteltaub^{1*}, E. Van der Giessen²

¹ Faculty of Aerospace Engineering, Delft University of Technology, The Netherlands

² Zernike Institute for Advanced Materials, University of Groningen, The Netherlands

ABSTRACT: A discrete dislocation-transformation model is used to analyze the response of an aggregate of ferritic and austenitic grains that can transform into martensite. In particular, the influence of the crystal orientation of the austenitic grains on the plastic and transformation behavior is studied. It is found that the austenitic crystal orientation has a stronger effect on the plastic behavior than on the transformation behavior. The transformation rate predicted by the discrete model only indicates a weak dependency on the austenitic crystal orientation.

KEYWORDS: Multiphase steels, martensitic transformation, discrete dislocation, crystallographic orientation

1 INTRODUCTION

Multiphase steels assisted by transformation induced plasticity, known as TRIP steels, are an important class of materials due to their good combination of strength and ductility. During mechanical loading, TRIP steels gain additional strength due to a martensitic transformation of the austenitic phase. This phenomenon is strongly coupled to plastic deformations in the surrounding phases. In order to optimize the mechanical properties of this class of steels, it is important to understand the coupling of the transformation and plasticity at various length scales. At sub-grain length scales, discrete models are particularly well-suited in order to analyze the details of the complex interaction between plasticity and transformation. In the present communication, a discrete model is used to analyze an aggregate of ferritic grains (that form the matrix of a multiphase steel) and dispersed grains of austenite that can partially transform into martensitic platelets upon loading, as shown schematically in Figure 1. The main goal of the present analysis is to study the effect of the crystal orientation of the austenitic grains.

2 DISCRETE MODEL

2.1 DECOMPOSITION

In the discrete dislocation-transformation model, plastic deformation is accounted for through discrete dislocations (identified with an index i) whereas transformation is modeled through individual martensitic plates (identified with an index k). Following the approach developed in [1], the stress σ , strain ϵ and displacement u are de-

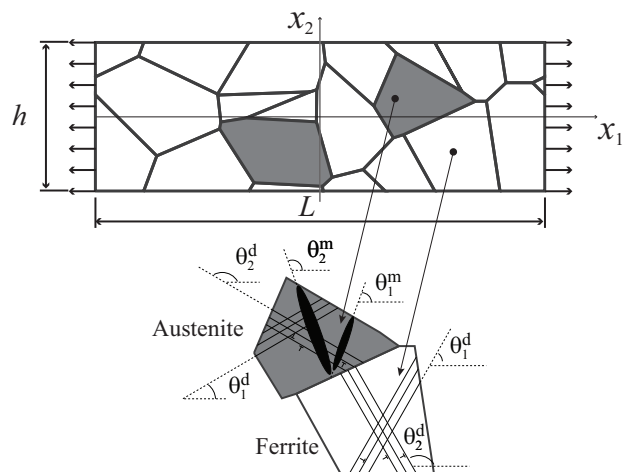


Figure 1: Two-dimensional model of an aggregate of ferrite and austenite grains. The martensite that forms upon transformation of austenite is shown in dark gray.

composed as follows:

$$\begin{aligned}\sigma &= \sigma^m + \sigma^d + \sigma^c, \\ \epsilon &= \epsilon^m + \epsilon^d + \epsilon^c, \\ u &= u^m + u^d + u^c,\end{aligned}\tag{1}$$

where the superscripts m, d and c refer to a transformation problem, a dislocation problem and a complementary problem, respectively.

The transformation problem consists of isolated platelets of martensite embedded in an infinite austenitic matrix and subjected to a transformation strain ϵ_k^{tr} (due to the formation of martensitic plate k) given by

$$\epsilon_k^{\text{tr}} = \frac{1}{2} \gamma (\mathbf{m}_k^\perp \otimes \mathbf{m}_k + \mathbf{m}_k \otimes \mathbf{m}_k^\perp) + \delta (\mathbf{m}_k \otimes \mathbf{m}_k). \tag{2}$$

*Corresponding author: Faculty of Aerospace Engineering, Delft University of Technology, Kluyverweg 1, 2629 HS Delft, The Netherlands, S.R.Turteltaub@tudelft.nl

Here, the vector \mathbf{m}_k is the unit normal to the (nominal) habit plane, \mathbf{m}_k^\perp is a vector along the (nominal) habit plane, δ is the normal expansion and γ is the shear parallel to the habit plane (see e.g., [2] for details). Analytical expressions for the case of martensitic plates with elliptical cross-sections and edge dislocations in an isotropic medium can be found in [1] and [3], respectively.

The dislocation problem refers to dislocations embedded in an infinite homogeneous medium (either ferrite, austenite or martensite depending on the phase in which the dislocation core is located).

The complementary field, which is obtained numerically, is used to satisfy the actual boundary conditions and to account for the inhomogeneities due to the presence of a ferritic matrix as well as the formation and growth of martensitic plates. The tensor of elastic moduli of a phase p is denoted as \mathbb{C}^p , with $p = f, a$ or m for the ferritic, austenitic or martensitic phases, respectively. For an isotropic phase,

$$\mathbb{C}^p = \frac{1}{3}(3\kappa^p - 2\mu^p)\mathbf{I} \otimes \mathbf{I} + 2\mu^p\mathbb{I}, \quad (3)$$

where κ^p is the bulk modulus, μ^p is the shear modulus, and \mathbf{I} and \mathbb{I} are the second and fourth-order identity tensors, respectively. Under quasi-static conditions, the complementary boundary value problem corresponds to solving $\text{div} \boldsymbol{\sigma}^c = \mathbf{0}$, together with the following stress-strain relations:

$$\boldsymbol{\sigma}^c = \begin{cases} \mathbb{C}^f \boldsymbol{\varepsilon}^c + \mathbf{P}_f^d & \text{in ferrite} \\ \mathbb{C}^a \boldsymbol{\varepsilon}^c + \mathbf{P}_a^d & \text{in austenite} \\ \mathbb{C}^m \boldsymbol{\varepsilon}^c + \mathbf{P}_k^d + \mathbf{P}_k^m & \text{in martensitic plate } k \end{cases} \quad (4)$$

with $\boldsymbol{\varepsilon}^c = \frac{1}{2}(\nabla \mathbf{u}^c + (\nabla \mathbf{u}^c)^T)$ and prescribed boundary conditions for the complementary fields that follow from the boundary conditions of the original problem upon using (1). In (4), the tensors \mathbf{P}_f^d , \mathbf{P}_a^d , \mathbf{P}_k^m and \mathbf{P}_k^d are polarization stresses that result from the difference in elastic properties between the ferrite, austenite and martensite. The subscripts f , a and k indicate that the polarization stresses are used to correct for the proper stiffness in the ferritic, austenitic or martensitic regions, respectively, while the superscripts m and d indicate that the polarization stresses are related to the martensitic transformation or to the dislocation field, respectively. Expressions for these tensors in the case of a single crystal of austenite can be found in [1] and will be presented in detail for the case of multiphase steels in a forthcoming publication of the present authors.

2.2 EVOLUTION OF MICROSTRUCTURE

Based on the stress state at a given time, evolution relations are used to update the number and location of martensitic plates and dislocations for subsequent times. Referring to [1] for further details, these rules are briefly summarized here for the two-dimensional problem at hand (Figure 1), in which all dislocations are of edge character. The appearance of new dislocation dipoles and martensitic plates is simulated using nucleation sources randomly distributed across the specimen (dislocation sources in fer-

rite and austenite and transformation sources in austenite). At each transformation source k , a nominal driving force (based on the nominal habit plane) is compared with a critical value f_k^{cr} . If the critical value is exceeded, possible nucleation of martensite is further tested based on an embryonic plate centered at the source and with a major semi-axis of length c_0 . The final criterion to allow the actual nucleation of an embryonic martensitic plate is that it can grow, based on the following growth model: Growth of a martensitic plate is assumed to occur by lateral movement of the tips of the elliptical cross section along the (nominal) habit plane (i.e., major axis of cross section). In the present model, it is assumed that the aspect ratio of the martensitic plates is preserved during growth. Consequently, the growth of the plate can be specified based on the velocities of the tips, denoted as $v_t^{(1)}$ and $v_t^{(2)}$. The kinetic law that relates the velocity of tip $q = 1, 2$ to an effective transformation driving force can be expressed as

$$v_t^{(q)} = \frac{1}{B_m (\pi e c)^2} \int_{S_k^m} f_k^{\text{tr}} w^{(q)} \text{d}s \quad (q = 1, 2), \quad (5)$$

where B_m is a drag coefficient for transformation, e is the aspect ratio of the martensitic plate, c is the length of the major semi-axis, S_k^m is the interface between the martensitic platelet and the austenite, f_k^{tr} is the (local) transformation driving force at points on S_k^m and $w^{(q)}$ is a weighting function that varies from 1 at tip q to 0 at the opposite tip. An expression for the local value of the driving force f_k^{tr} can be found in [1]. The actual value of the tip velocity is limited by a cut-off value v_{max}^m i.e., $0 \leq v_t^{(q)} \leq v_{\text{max}}^m$ for $q = 1, 2$. Additional rules to handle special situations can be found in [1].

Nucleation of dislocation dipoles is modeled by two-dimensional Frank-Read sources and is controlled by the Peach-Koehler force f^d (dislocation driving force). A dislocation dipole is nucleated when the magnitude $|f^d|$ of the Peach-Koehler force exceeds a critical value $f^{\text{cr}} = b\tau^{\text{cr}}$ during a prescribed time interval t_{nuc} . Here, b is the magnitude of the Burgers vector and τ^{cr} is a critical resolved shear stress at a source. After nucleation, the movement of each dislocation core i is determined by its velocity v_i^d , which is specified using the following kinetic relation with the Peach-Koehler force f_i^d acting on dislocation i :

$$v_i^d = \frac{f_i^d}{B_d}, \quad 0 \leq v_i^d \leq v_{\text{max}}^d, \quad (6)$$

where v_i^d is the velocity of the dislocation along the slip direction, B_d is a drag coefficient and v_{max}^d is a cut-off value for the dislocation velocity. Additional details can be found in [3].

The nucleation criterion and kinetic law used for the ferrite and the austenite are formally similar (only the values of the model parameters are distinct). Experimental evidence indicates that in high-carbon martensite the behavior is mostly elastic until fracture, which occurs at high stress levels (see [4]). Consequently, Frank-Read sources

Table 1: Parameters for polycrystal simulations (overbars indicate mean of Gaussian distribution and SD denotes standard deviation). Unless explicitly indicated, dislocation parameters for the ferrite and austenite are taken equal to each other.

Ferrite	$\kappa^f = 200 \text{ GPa}, \mu^f = 66.7 \text{ GPa}$
Austenite	$\kappa^a = 200 \text{ GPa}, \mu^a = 66.7 \text{ GPa}$
Martensite	$\kappa^m = 260 \text{ GPa}, \mu^m = 86.7 \text{ GPa}$
Trans. strain	$\delta = 4 \cdot 10^{-3}, \gamma = 2 \cdot 10^{-2}$
Source strength	$\bar{f}_k^{\text{cr}} = 4 \text{ MPa}, \text{SD} = 0.8 \text{ MPa}$
Embryonic plate	$c_0 = 0.1 \mu\text{m}, e = 0.125$
Trans. kinetic law	$B_m = 10^8 \text{ Pa} \cdot \text{s} \cdot \text{m}^{-2}$ $v_{\text{max}}^m = 4800 \text{ m} \cdot \text{s}^{-1}$
Burgers vector	$b = 0.25 \text{ nm}$
Nucleation time	$t^{\text{nuc}} = 10 \text{ ns}$
Strength ferrite	$\bar{\tau}^{\text{cr}} = 150 \text{ MPa}, \text{SD} = 30 \text{ MPa}$
Strength austenite	$\bar{\tau}^{\text{cr}} = 170 \text{ MPa}, \text{SD} = 34 \text{ MPa}$
Disl. kinetic law	$B_d = 10^{-4} \text{ Pa} \cdot \text{s}$ $v_{\text{max}}^d = 20 \text{ m} \cdot \text{s}^{-1}$

originally located in the austenitic phase that, due to a phase transformation, become embedded in the martensitic phase, are deactivated. Grain boundaries are incorporated in the simulation as impenetrable barriers for the movement of dislocations and, in the case of austenite-ferrite boundaries, as barriers for the growth of martensitic plates.

3 SIMULATIONS

The present simulations are carried out within a plane strain setting, hence attention is restricted to the movement of edge dislocations whose dislocation lines lie in the out-of-plane direction of the specimens. Two slip planes, with plane normals forming an angle of 60° between them, are used inside the ferritic and austenitic phases, while two habit plane normal vectors \mathbf{m}_k in the austenitic phase are chosen oriented at angles of 40° and 80° with respect to the austenitic slip plane normals. Values for geometrical and material parameters are indicated in Table 1 (see [1] for additional explanations).

In all simulations, a rectangular sample with in-plane dimensions $L = 12 \mu\text{m}$ and $h = 4 \mu\text{m}$ (cf. Figure 1) is subjected to plane-strain uniaxial deformation by imposing the following boundary conditions: $u_1 = \pm(1/2)L\dot{\epsilon}t$ and $u_2 = 0$ for $x_1 = \pm L/2$ and $\sigma_{12} = \sigma_{22} = 0$ for $x_2 = \pm h/2$, with a nominal strain rate $\dot{\epsilon} = \pm(1/6) \cdot 10^4 \mu\text{m} \cdot \text{s}^{-1}$. The left and right sides of the specimen are taken to be impenetrable boundaries for dislocations. The top and bottom sides of the samples are free surfaces across which dislocations can move out of the specimen. Two uniform orientations of the austenitic grains are analyzed as indicated in Table 2 in terms of the slip and transformation systems (see also Figure 1). Observe that orientation A is symmetric with respect to the tensile direction. The angles θ_1^d and θ_2^d for the ferritic grains are chosen randomly. For

Table 2: Orientation of slip and transformation systems of austenite (angles are measured anti-clockwise with respect to the sample's loading axis).

Austenitic orientation	θ_1^d	θ_2^d	θ_1^m	θ_2^m
Orientation A	30°	150°	70°	110°
Orientation B	340°	100°	20°	60°

each austenitic orientation, two cases are studied: a simulation with dislocation sources only (Case 1) and a simulation with dislocation and transformation sources (Case 2). The first case represents a non-transforming mixture of ferrite and austenite and the second case corresponds to a mixture of ferrite, austenite and martensite, which represents the transformation-induced plasticity case.

Figure 2 shows the average axial stress $\bar{\sigma}_{11}$ as a function of the average axial strain $\bar{\epsilon}_{11}$ of the samples with orientations A and B for the cases with and without transformation. The strengthening effect due to transformation-

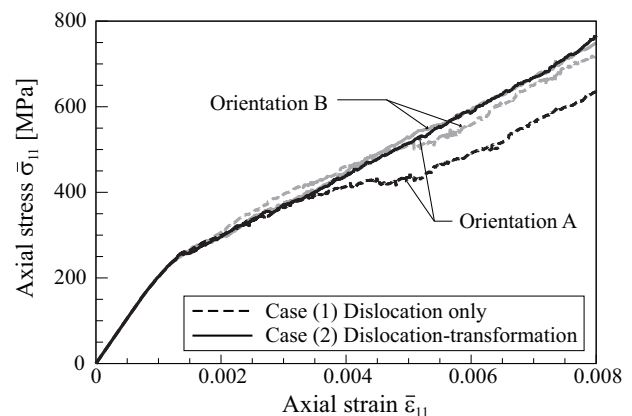


Figure 2: Average axial stress $\bar{\sigma}_{11}$ as a function of the average axial strain $\bar{\epsilon}_{11}$ of the samples with orientations A and B for the cases with and without transformation.

induced plasticity can be observed by comparing the dislocation-only case (dashed line) with the combined dislocation-transformation case (solid line). The strength of the combined dislocation-transformation case is initially slightly smaller than the dislocation-only case due to the additional stress relaxation connected to the martensitic transformation. However, after transformation has occurred, the strength of the dislocation-transformation case increases above the dislocation-only case, signaling the increased influence of the (hard) martensitic phase. For orientation A (symmetrically-oriented) this effect is more significant than for orientation B. Interestingly, the stress responses of the combined dislocation-transformation case for orientations A and B are similar; the main effect of the crystal orientation seems to be on the dislocation-only case. In particular, the stress curve for orientation A in the dislocation-only case shows a softer response than the corresponding dislocation-only case for orientation B.

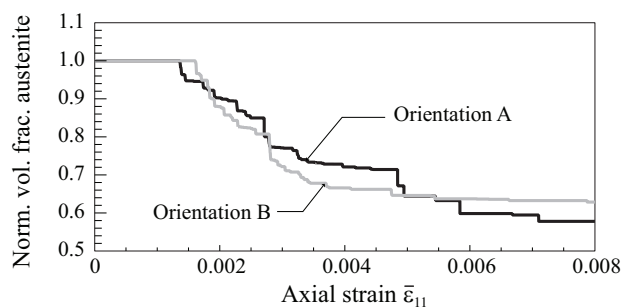


Figure 3: Normalized volume fraction of austenite as a function of the average axial strain $\bar{\varepsilon}_{11}$ of the samples with orientations A and B.

The normalized transformation fraction (i.e., the current value of volume fraction of austenite divided by the initial value of the volume fraction) is shown in Figure 3. The average transformation rate for orientation B is slightly lower than for orientation A, which is consistent with a priori predictions based on a nominal transformation driving force and a homogeneous state of uniaxial tension. Nevertheless, the transformation rates are in general terms somewhat similar, hence the present simulations indicate that the effect of orientation on transformation rate is relatively weak. This weak dependency can be interpreted in terms of the actual stress field in the computations, which deviate considerably from uniaxial tension. Indeed, the fluctuations in axial stress within the sample can be significant, as shown in Figure 4, which depicts the distribution of σ_{11} at an axial strain of $\bar{\varepsilon}_{11} = 0.65\%$ for orientations A and B. From this figure, which corresponds to a state where significant transformation has occurred, it can be seen that the stress fields in the ferritic matrix for orientations A and B are relatively similar, which is consistent with the similar stress-strain response for the combined cases as shown in Figure 2. This similarity can be explained as follows: Due to dislocation pile-ups on the ferritic grains adjacent to the austenitic grains, the transformation driving force is sufficiently large to trigger the nucleation of martensite for both orientations A and B. Furthermore, once the austenitic grains have significantly transformed into martensite, the subsequent response is similar for both orientations since (i) the elastic behavior of the martensite is assumed to be isotropic and (ii) the plastic deformation on the untransformed austenite only plays a minor role. It is plausible that the effect of the austenitic grain orientation might be stronger if elastic anisotropy is also incorporated in the modeling, but such formulation lies outside of the scope of the present work.

4 CONCLUSIONS

The austenitic grain orientation appears to have a stronger effect on the plastic deformation than on the martensitic transformation. Even though orientation B is nominally less favorable for transformation than the symmetrically-oriented configuration A for a homogeneous state of uniaxial stress, the transformation rates are somewhat simi-

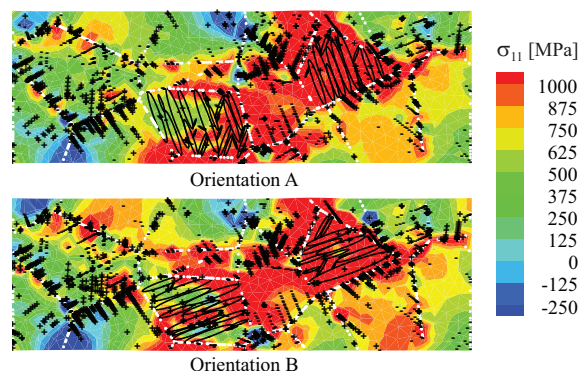


Figure 4: Contour plot of axial stress σ_{11} for a total strain of $\bar{\varepsilon}_{11} = 0.65\%$ for orientation A (above) and orientation B (below).

lar for both cases. The discrete dislocation-transformation simulations reveals that the stress field is sufficiently heterogeneous at the sub-micron scale to activate transformation sources that would normally not be activated under locally more homogeneous conditions (see e.g., [2]). This information is relevant for mesoscale models in the sense that stress concentrations (such as pile-ups at grain boundaries) turn out to play a significant role on the transformation behavior and therefore need to be taken into account.

ACKNOWLEDGEMENT

This research was carried out under project number MC2.03177 in the framework of the Research Program of the Materials innovation institute M2i (www.m2i.nl).

REFERENCES

- [1] J. Shi, S. Turteltaub, E. Van der Giessen, and J. J. C. Remmers. A discrete dislocation–transformation model for austenitic single crystals. *Modelling Simul. Mater. Sci. Eng.*, 16(5), 2008. doi: 10.1088/0965-0393/16/5/055005.
- [2] S. Turteltaub and A. S. J. Suiker. A multi-scale thermomechanical model for cubic to tetragonal martensitic phase transformations. *Int. J. Solids Struct.*, 43:4509–4545, 2006.
- [3] E. Van der Giessen and A. Needleman. Discrete dislocation plasticity: a simple planar model. *Modelling Simul. Mater. Sci. Eng.*, 3(5):689–735, 1995.
- [4] P. J. Jacques, Q. Furnémont, S. Godet, T. Pardoen, K.T. Conlon, and F. Delannay. Micromechanical characterisation of trip-assisted multiphase steels by in situ neutron diffraction. *Philos. Mag.*, 86(16): 2371–2392, 2006.